The Astrophysical Journal, 628:L113–L117, 2005 August 1
© 2005. The American Astronomical Society. All rights reserved. Printed in U.S.A.

THE ARCHES CLUSTER: EVIDENCE FOR A TRUNCATED MASS FUNCTION?[1]

Andrea Stolte,[2,3] Wolfgang Brandner,[2] Eva K. Grebel,[2,4] Rainer Lenzen,[2] and Anne-Marie Lagrange[5]

Received 2004 October 11; accepted 2005 June 22; published 2005 July 18

ABSTRACT

We have analyzed high-resolution, adaptive optics *HK* observations of the Arches cluster obtained with NAOS-CONICA. With a spatial resolution of 84 mas, the cluster center is uniquely resolved. From these data, the present-day mass function (MF) of the Arches cluster is derived down to ~4 $M_\odot$. The integrated MF and the core and second-annulus MFs are consistent with a turnover at 6–7 $M_\odot$. This turnover indicates severe depletion of intermediate- and low-mass stars in the Arches cluster, possibly caused by its evolution in the Galactic center environment. The Arches MF represents the first resolved observation of a starburst cluster exhibiting a low-mass–truncated MF. This finding has severe implications for stellar population synthesis modeling of extragalactic starbursts, the derivation of integrated properties such as the total mass of star clusters in dense environments, the survival of low-mass remnants from starburst populations, and chemical enrichment during starburst phases.

Subject headings: Galaxy: center — open clusters and associations: individual (Arches) — stars: luminosity function, mass function — techniques: high angular resolution

Online material: color figure

1. INTRODUCTION

The Arches cluster is one of the rare compact starburst clusters forming in the Milky Way today. At a projected distance of only 25 pc from the Galactic center (GC), it forms a unique template for star and cluster formation in the nuclei of external galaxies. Even at an age of only 2 Myr, its elongated shape evidences the strong tidal forces acting to disrupt the compact starburst cluster despite its large central density of $3 \times 10^5\ M_\odot\ \mathrm{pc}^{-3}$ (Figer et al. 1999). *N*-body simulations suggest that clusters in the GC environment will dissolve on timescales as short as 10 Myr (Kim et al. 2000; Portegies Zwart et al. 2002). This leaves us with very few clusters available to study nearby, spatially resolved starburst clusters, especially at the Milky Way's present low cluster formation rate.

The Arches cluster is known to be heavily mass-segregated, with a flat present-day MF ($\Gamma \sim 0$, where the Salpeter slope is $\Gamma = -1.35$) in the cluster core ($r_{\mathrm{core}} = 0.2$ pc at a distance of 8 kpc) (Stolte et al. 2002; Figer et al. 1999). The concentration of high-mass stars in the cluster core causes the integrated MF to be flattened with respect to a Salpeter MF, with a slope of $\Gamma \sim -0.9$ to -1.1 depending on the radial selection of the cluster area (Stolte 2003). In this Letter, we derive the present-day MF of the Arches cluster from adaptive optics (AO) data with a spatial resolution of 0.″084. This constitutes the currently deepest photometry of the cluster core with the highest spatial resolution, which allows us to derive the present-day MF down to ~5 $M_\odot$ in the cluster core ($r < 0.2$ pc) and 2 $M_\odot$ at larger radii.

2. OBSERVATIONS AND DATA REDUCTION

NAOS-CONICA (NACO) is the ESO VLT facility AO system with its infrared camera. NAOS is a 189-element Shack-Hartmann AO system with two wave-front sensors operating in the visual and near-infrared (Rousset et al. 2003). CONICA is a 1–5 μm imaging camera and spectrograph designed for diffraction-limited observations with the VLT 8 m mirror (Lenzen et al. 2003).

The Arches cluster ($\alpha = 17^{\mathrm{h}}45^{\mathrm{m}}50^{\mathrm{s}}$, $\delta = -28°49'28''$; J2000) was observed during the NACO commissioning phase in 2002 March to probe the AO crowded-field performance. The medium-resolution camera (0.″027 pixel^{-1}) optimized for *K*-band observations was used, covering a field of view of 27″. A foreground star with $V \sim 16$ mag close to the cluster served as the guide source. Moderate Strehl ratios of 14% in *H* band and 20% in *K* band were achieved, resulting in a resolution of 0.″084 in both filters. Integration times were 14 minutes in *H* and 7 minutes in K_s. The detection limits on the combined images shown in Figure 1 were $K_s < 20.5$ and $H < 22$ mag.

Standard data reduction was performed under IRAF, images were combined using Drizzle with 2 × 2 oversampling to enhance source detection, and point-spread function (PSF) fitting photometry was obtained with DAOPHOT. The isoplanatic patch was large during the observations, such that no elongation of the PSF at larger distances from the guide star due to anisoplanatism is observed. *Hubble Space Telescope* (*HST*) Near Infrared Camera and Multi-Object Spectrometer (NICMOS) observations of the Arches cluster (Figer et al. 1999) were used to probe the stability of the photometric correction and derive a uniform photometric calibration over the NACO field. The calibration procedure is described in detail with respect to Gemini/Hokupa'a data on the cluster in Stolte et al. (2002). In the case of the NACO data, the zero point was constant and no color terms were found. In the following, all magnitudes are shown in the *HST* NICMOS system, with *K* corresponding to the F205W NICMOS broadband filter, and *H* to F160W. All isochrones are transformed into the NICMOS system accordingly (Brandner et al. 2001).

[1] Based on NAOS-CONICA commissioning observations obtained at the ESO Very Large Telescope, on Cerro Paranal, Chile.

[2] Max-Planck-Institut für Astronomie, Königstuhl 17, D-69117 Heidelberg, Germany; brandner@mpia.de, lenzen@mpia.de.

[3] University of Florida, 211 Bryant Space Science Center, Gainesville, FL 32111-2055; stolte@astro.ufl.edu.

[4] Astronomisches Institut, Universität Basel, Venusstrasse 7, CH-4102 Binningen, Switzerland; grebel@astro.unibas.ch.

[5] Laboratoire d'Astrophysique, Observatoire de Grenoble, B.P. 53, F-38041 Grenoble Cedex 9, France; anne-marie.lagrange@cnrs-dir.fr.

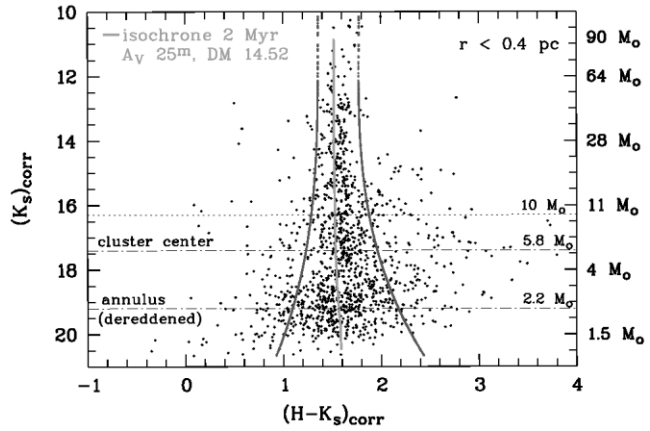


FIG. 2.—Differential extinction–corrected CMD of the Arches cluster. The 2 Myr Geneva isochrone used to derive the MF is shown as the solid central line. The color cut used to reject foreground and background contamination (*enveloping lines*) widens according to the increasing photometric uncertainty at fainter magnitudes. The 50% incompleteness limits in the cluster core and the second annulus (0.2 pc $< r <$ 0.4 pc) are shown as dashed lines, and masses are labeled as derived from the isochrone displayed. The radial selection to $r < 10''$, or 0.4 pc, minimizes field star contamination.

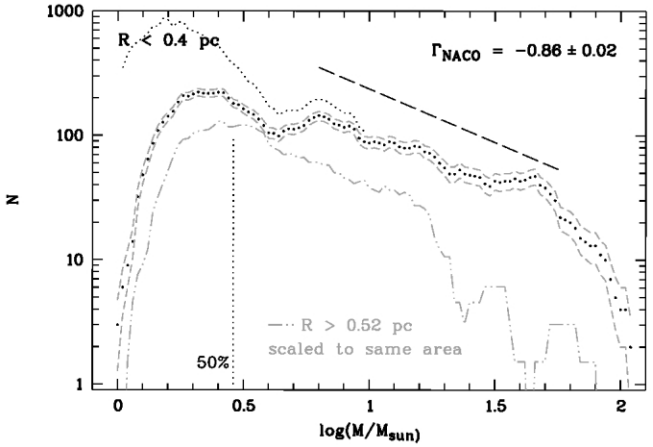


FIG. 3.—Present-day MF as derived from a 2 Myr Geneva isochrone applied to the CMD shown in Fig. 2. A bin width of $\Delta \log (M/M_\odot) = 0.2$ and bin shift of $\delta \log (M/M_\odot) = 0.02$ were used to obtain individual number counts. The gray enveloping lines denote the Poisson uncertainty for each point. The slopes and fitting uncertainties are derived from a weighted, linear least-squares fit over the range $6\ M_\odot < M < 60\ M_\odot$ (*dashed black line*). The high-mass MF is, with $\Gamma = -0.86$, moderately flattened with respect to a Salpeter IMF ($\Gamma = -1.35$), indicating a bias to high-mass objects, and displays a turnover at $\log (M/M_\odot) = 0.8$, or $M = 6\ M_\odot$. An upper limit to the possible field star contamination (*dash-dotted line*) derived from the outer NACO field indicates that field stars are dominant below $\log (M/M_\odot) = 0.6$, or $4\ M_\odot$.

2.1. *Artificial-Star Simulations*

The completeness in the crowding-limited cluster field was derived from the recovery fraction of artificial stars. In order to avoid changes in the local stellar density, only 200 stars were inserted per frame on a total of 100 frames, or 20,000 stars. The same stars randomly inserted into the *K*-band frame were transformed to instrumental *H*-band magnitudes using the characteristic Arches main-sequence color of $H-K = 1.63$ mag. This is important because only stars detected in both *H* and *K* simultaneously enter the MF calculation. PSF photometry was derived in the same way as the original photometry. Recovered stars were selected by uncertainty and color in the same way as real stars entering the MF. The recovery fraction is determined for each annulus individually, such that increasing crowding effects at smaller radii are taken into account. In the cluster core, the stellar density is significantly higher than in the outer annuli. The simulations showed that inserted bright stars influence the recovery fraction of fainter stars severely. Therefore, the core field with the highest stellar density was excerpted from the NACO field. On this excerpt, only 10 stars within bins of 1 mag were added on 100 artificial frames, leading to 1000 stars per magnitude bin. For the core number counts ($r < 0.2$ pc), only the recovery fraction from the core simulation was used.

3. THE ARCHES CLUSTER PRESENT-DAY MASS FUNCTION

Prior to the mass determination, stellar magnitudes and colors were corrected for the systematic variation in extinction observed over the Arches field (Stolte et al. 2002). Foreground and background sources were rejected by applying a color cut as shown in Figure 2. The increasing photometric uncertainty toward fainter stars as indicated by artificial-star tests was taken into account by widening the color selection toward fainter magnitudes. Because of the location in the dense GC region, field contamination increases toward fainter magnitudes. This is apparent in the increase of blue foreground and red background sources in the color-magnitude diagram (CMD) below $K = 15.5$ mag (14 $M_\odot$), while contamination at higher masses is negligible. A dense concentration of bulge stars can be seen at the faint end, $K > 18$ mag, which is beyond the 50% completeness limit in the MF and does not affect the MF fit. Field contamination becomes particularly important beyond a radius of $10''$. As no background field is available, the MF is limited to radii $r < 10''$, or 0.4 pc, twice the core radius of 0.2 pc (Stolte et al. 2002), to minimize field contamination. As some field star component is still present in the radial and color selection, this results in a conservative upper limit to the flattened MF.

The present-day MF was derived from the corrected CMD (Fig. 2), converting *K*-band magnitudes into masses using a 2 Myr Geneva main-sequence isochrone (Lejeune & Schaerer 2001) with solar metallicity.[6] A distance modulus of 14.52 mag and foreground extinction of $A_V = 25.2$ mag were applied to the isochrone, and reddened luminosities were transformed into the NICMOS system using color equations derived from comparison of five NICMOS standards and reddened stars in the Arches field with the Two Micron All Sky Survey. Present-day masses were used, as present-day properties are calibrated against observations while the recalculation to initial masses is heavily dependent on the mass-loss model. No correction was made for stellar evolution, which affects only stars above 50 $M_\odot$ [$\log (M/M_\odot) \geq 1.7$], to avoid uncertainties in stellar evolution modeling of very massive stars.

Stars were counted in magnitude intervals of $\Delta \log (M/M_\odot) = 0.2$. In order to minimize binning effects, 10 MFs were calculated with bins shifted by $\delta \log (M/M_\odot) = 0.02$. The points from all 10 calculations are included to yield the present-day MF presented in Figure 3. The advantage of this method lies in the fact that features in the MF are not erased as a consequence of binning, and that the resultant MF fit is statistically more significant. A linear least-squares fit was performed to obtain the slopes. The true uncertainty in the derived MF

[6] The metallicity in the high-mass component of the Arches cluster was recently found to be solar (Najarro et al. 2004), while supersolar-metallicity isochrones were used in earlier studies (see discussion in Figer et al. 1999; Stolte et al. 2002; Stolte 2003).

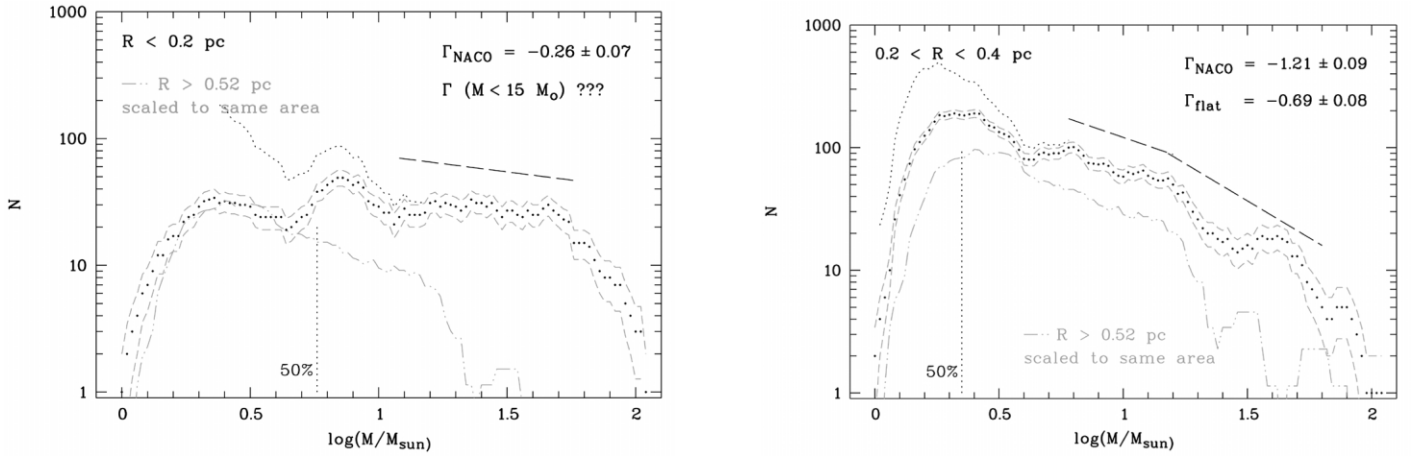


FIG. 4.—Mass segregation and turnover in the Arches cluster core. The core MF ($r < 0.2$ pc, *left*) is heavily biased to high-mass stars, with a pronounced TO at $\log (M/M_\odot) = 0.84$, or 7 $M_\odot$. The linear least-squares fit (*dashed black line*) shows that the MF steepens from $\Gamma \sim -0.26$ (12 $M_\odot < M < 60$ $M_\odot$) to a Salpeter-like slope of $\Gamma = -1.21$ (16 $M_\odot < M < 60$ $M_\odot$) at the high-mass end and $\Gamma = -0.69$ (6 $M_\odot < M < 16$ $M_\odot$) for intermediate masses in the second annulus (0.2 pc $< r <$ 0.4 pc, *right*), while the TO is still present around 6 $M_\odot$. The area-scaled MF of the outer NACO field ($r > 0.5$ pc) indicates that the TO becomes more pronounced when field data are available. The similar TO mass in both annuli contradicts expectations from dynamical segregation and supports a low-mass–depleted IMF in the Arches cluster.

slope is larger than the formal fit uncertainty and is dominated by the choice of the isochrone, the photometric uncertainties of individual stars, and individual extinction. We estimate the true uncertainty in Γ to be ± 0.15 from experimenting with different fitting ranges and isochrone parameters (metallicity, age; see Stolte 2003 for details).

The most striking feature in the present-day MF of the Arches cluster (Fig. 3) is a change in the sign of the MF slope at $\sim$6 $M_\odot$ indicative of a turnover (TO). The MF has therefore been fitted in the mass range 6 $M_\odot < M <$ 60 $M_\odot$ [$\log (M/M_\odot) > 0.8$]. The MF is, with a slope of $\Gamma = -0.86$, moderately flattened with respect to the Salpeter value of $\Gamma = -1.35$. This slope is in very good agreement with previous values of $\Gamma = -0.77$ derived from *HST* NICMOS data (Figer et al. 1999; Stolte et al. 2002), and $\Gamma = -0.82$ derived from Gemini/Hokupa'a data (Stolte 2003). Below 6 $M_\odot$ [$\log (M/M_\odot) < 0.8$], the MF deviates from a power law, but it appears to *decrease* toward lower masses in the interval $0.6 < \log (M/M_\odot) < 0.8$. Around 4 $M_\odot$, the increase in the apparent MF is likely caused by the increasing contribution of field stars.

As field contamination increases with decreasing mass, especially for masses below $\sim$10 $M_\odot$ ($K = 16.3$ mag), the observed TO will be enhanced when field stars are subtracted. As an upper limit to the field star contribution, we consider stars close to the edge of the NACO field, at cluster radii $r >$ 13″ (0.5 pc). The corresponding apparent MF, scaled to the same area (Fig. 3, *dash-dotted line*), suggests that the population is dominated by field stars or segregated low-mass cluster members below 3 $M_\odot$, while the high-mass end above 15 $M_\odot$ is entirely dominated by cluster stars. Between 3 and 15 $M_\odot$, the range where the TO occurs, field stars may contribute as much as 50%. The discrepancy between the high- and the intermediate-mass regime in the Arches MF will therefore become more pronounced as soon as proper field star estimates are available. The TO in the MF is supported by the fact that no evidence of such a feature is observed in the outer field population, as would be expected if field star contamination introduced this feature into the MF.

Two possibilities can be envisioned to explain the flattening in the Arches MF. The MF either could be truncated at the low-mass end, which would imply that the dense GC environment has severe impacts on the local *initial* MF (IMF), or the tidal forces acting on the cluster could have caused rapid dynamical segregation on timescales as short as 2 Myr. Such dynamical evolution would transport massive stars into the core and low-mass stars to larger radii. The dynamical timescales for an Arches-like cluster are suggested to be as short as a few million years from *N*-body simulations (Kim et al. 2000; Portegies Zwart et al. 2002), such that dynamical disruption has likely contributed to the observed spatial distribution of cluster stars.

4. THE MASS FUNCTION TURNOVER IN TWO ANNULI

In the case of dynamical segregation, the apparent high-mass TO would be a feature of the cluster core, where the massive stars accumulate, while stars with lower masses are ejected. The median mass is expected to decrease with distance from the cluster center. If the median mass is evidenced in the TO, the TO mass should also shift toward lower masses at larger radii. The core ($r < 0.2$ pc) and second-annulus (0.2 pc $< r <$ 0.4 pc) MFs are compared in Figure 4. While the core and second-annulus MFs significantly vary in shape, the TO is present at $\log (M/M_\odot) \sim 0.84$, or 7 $M_\odot$, in the core and at $\log (M/M_\odot) \sim 0.8$, or 6 $M_\odot$, in the second annulus, in both cases above the 50% completeness threshold and thus only marginally higher in the core. Although the TO appears much more pronounced in the core, the TO mass is *not* shifted significantly to lower masses in the second annulus, as would be expected from dynamical evolution alone. The constant TO mass in the inner and outer cluster supports the suggestion of a heavily low-mass–depleted *IMF* in the Arches cluster.

Above 6 $M_\odot$, both MFs differ significantly. The core MF features a power law with a flat slope, $\Gamma = -0.26$, indicating very efficient production of high-mass stars in the Arches core. The sharp transition toward a flat MF above 10 $M_\odot$ lets us speculate that a distinct physical process influences the formation of high-mass stars, arguing for primordial segregation. Such a scenario is consistent with the requirement of an exceptionally dense environment to form the most massive stars. The MF slope in the second annulus steepens to a Salpeter power law with $\Gamma = -1.21$ for $M > 16$ $M_\odot$, while intermediate-mass stars are still overabundant, as indicated by a flattened

MF with $\Gamma = -0.7$ for 6 $M_\odot < M <$ 16 $M_\odot$. Before field contamination starts to dominate at 4 $M_\odot$, the MF flattens to $\Gamma \sim 0$ below 6 $M_\odot$.

A Kolmogorov-Smirnov (K-S) test comparing the incompleteness-corrected cumulative mass functions (CFs) for $M >$ 6 $M_\odot$ yields a probability of less than 10^{-4} that the core and "field" ($r > 13''$) CFs are drawn from the same distribution, and 0.03 of the core compared with the second annulus. The probability of a common origin of the second annulus and field CFs is as high as 0.26, or 26%. The higher values derived for the second annulus indicate that the population at intermediate radii has some similarity to both the core and the field but resembles the field much more closely. The K-S test results support the core population's being distinct from mass distributions at all larger radii and, in view of the flat MF, strengthens the case for high-mass bias/low-mass depletion in the Arches core.

Indirect evidence for a low-mass–truncated MF has been found in young, massive clusters in the center of the starburst galaxy M82 (Rieke et al. 1993). From the mass-to-light ratio, a low-mass cutoff at 2–3 $M_\odot$ is deduced assuming a normal high-mass IMF (Smith & Gallagher 2001). Below 3 $M_\odot$, the low-mass MF in the Arches core is remarkably consistent with the area-scaled distribution of "field" stars in the cluster halo ($r > 0.5$ pc), possibly indicating the low-mass limit in the *IMF* in the GC. However, tidal stripping can also be responsible for the redistribution of low-mass stars into the cluster outskirts. Such an effect, if at work in the Arches cluster, could also be at work in M82.

5. SUMMARY AND DISCUSSION

We report direct evidence for a low-mass–depleted MF in a nearby starburst cluster. The present-day MF of the Arches cluster displays a turnover around 6–7 $M_\odot$. A strong bias to high-mass and against low- and intermediate-mass stars is observed in the cluster core, which could be caused by rapid dynamical segregation or the selective formation of high-mass stars at the cost of intermediate-mass members. Field stars appear to become dominant around a few solar masses, indicating that proper field star subtraction might cause a decreasing low-mass MF for $M < 4\ M_\odot$. The apparent decrease in the low-mass MF can be caused by either tidal stripping of stars below 6 $M_\odot$ due to tidal disruption of the cluster in the GC tidal field or a truncated *IMF* in the dense GC environment.

Star formation theories predict that the characteristic mass depends on the initial conditions of the molecular cloud core and its environment. For a cloud of temperature $T_{\rm cl}$ with an embedded core $T_{\rm core}$, the critical mass for cloud collapse is the Bonnor-Ebert mass, $M_{\rm BE} \approx 0.35[T_{\rm core}/(10\ {\rm K})]^2[n_{\rm H_2}T_{\rm cl}/(10^6\ {\rm ergs\ cm^{-3}})]^{-1/2}$ (Elmegreen 2000). In molecular clouds in the solar neighborhood, typical values of $n_{\rm H_2} = 10^4\ {\rm cm^{-3}}$, $T_{\rm cl} = 100$ K, and $T_{\rm core} = 10$ K result in a characteristic mass of $\sim$0.3 $M_\odot$. Star formation in the GC environment takes place under more extreme conditions. Increased temperatures and densities, turbulent pressure, and the influence of magnetic fields (Mouschovias 1991; Shu et al. 2004) may alter the outcome of the star formation process. In the central molecular zone, the average $T_{\rm core} = 70$ K and cloud pressures are higher as a result of turbulence (Morris & Serabyn 1996). Assuming the thermal pressure is enhanced by a factor of 10 yields a Bonnor-Ebert mass of $\sim$5 $M_\odot$. Following Shu et al. (2004), the same characteristic mass arises when taking into account a magnetic field with $B_0 = 100\ \mu$G (Morris & Serabyn 1996). Hence the TO in the Arches MF can be understood as a natural result of the extreme star-forming environment in the GC.

If a low-mass–depleted IMF can be confirmed for the Arches cluster, this implies that a low-mass–truncated and possibly flattened IMF could be more adequate in intense star-forming environments, especially when using stellar synthesis models to derive the underlying mass distribution and star formation history of star clusters and galaxies. While the integrated luminosity will still be determined by high-mass stars, the underlying population will contribute significantly less to the buildup of a Galactic field population of low-mass stars surviving throughout a Hubble time. Metal enrichment will appear enhanced when compared with the surviving low-mass population after a timescale of a few hundred million years to a few gigayears, as the fraction of high-mass stars expected from a standard IMF will underestimate the true number of massive stars that formed and evolved in a galaxy. These implications have to be taken into account in the derivation of the star formation histories and evolution of external galaxies, and especially in the extreme star-forming environments of distant galaxies in the early universe.

The question whether the Arches IMF was indeed truncated below a few solar masses, whether the GC environment caused an unusually high TO mass as compared with the low-mass TO at 0.2–0.5 $M_\odot$ observed in the Trapezium (Muench et al. 2002; Hillenbrand 1997), or whether the cluster's dynamical evolution in the GC tidal field can entirely account for the present-day MF can only be solved by investigating a large area around the cluster and detailed field observations at comparably high spatial resolution as the NACO data presented here.

A. S. acknowledges Director General Discretionary Fund grant support from ESO and wishes to thank MPIA and Hans-Walter Rix for being an unusually supportive thesis host. We thank our referee, Simon Portegies Zwart, for suggestions that helped clarify and enhance this Letter.

REFERENCES

Brandner, W., Grebel, E. K., Barbá, R. H., Walborn, N. R., & Moneti, A. 2001, AJ, 122, 858
Elmegreen, B. G. 2000, MNRAS, 311, L5
Figer, D. F., Kim, S. S., Morris, M., Serabyn, E., Rich, R. M., & McLean, I. S. 1999, ApJ, 525, 750
Hillenbrand, L. A. 1997, AJ, 113, 1733
Kim, S. S., Figer, D. F., Lee, H. M., & Morris, M. 2000, ApJ, 545, 301
Lejeune, T., & Schaerer, D. 2001, A&A, 366, 538
Lenzen, R., et al. 2003, Proc. SPIE, 4841, 944
Muench, A. A., Lada, E. A., Lada, C. J., & Alves, J. 2002, ApJ, 573, 366
Morris, M., & Serabyn, E. 1996, ARA&A, 34, 645
Mouschovias, T. Ch. 1991, in The Physics of Star Formation and Early Stellar Evolution, ed. C. J. Lada & N. D. Kylafis (Dordrecht: Kluwer), 61
Najarro, F., Figer, D. F., Hillier, D. J., & Kudritzki, R. P. 2004, ApJ, 611, L105
Portegies Zwart, S. F., Makino, J., McMillan, S. L. W., & Hut, P. 2002, ApJ, 565, 265
Rieke, G. H., Loken, K., Rieke, M. J., & Tamblyn, P. 1993, ApJ, 412, 99
Rousset, G., et al. 2003, Proc. SPIE, 4839, 140
Shu, F. H., Li, Z.-Y., & Allen, A. 2004, ApJ, 601, 930
Smith, L. J., & Gallagher, J. S., III. 2001, MNRAS, 326, 1027
Stolte, A. 2003, Ph.D. thesis, Univ. Heidelberg
Stolte, A., Grebel, E. K., Brandner, W., & Figer, D. F. 2002, A&A, 394, 459

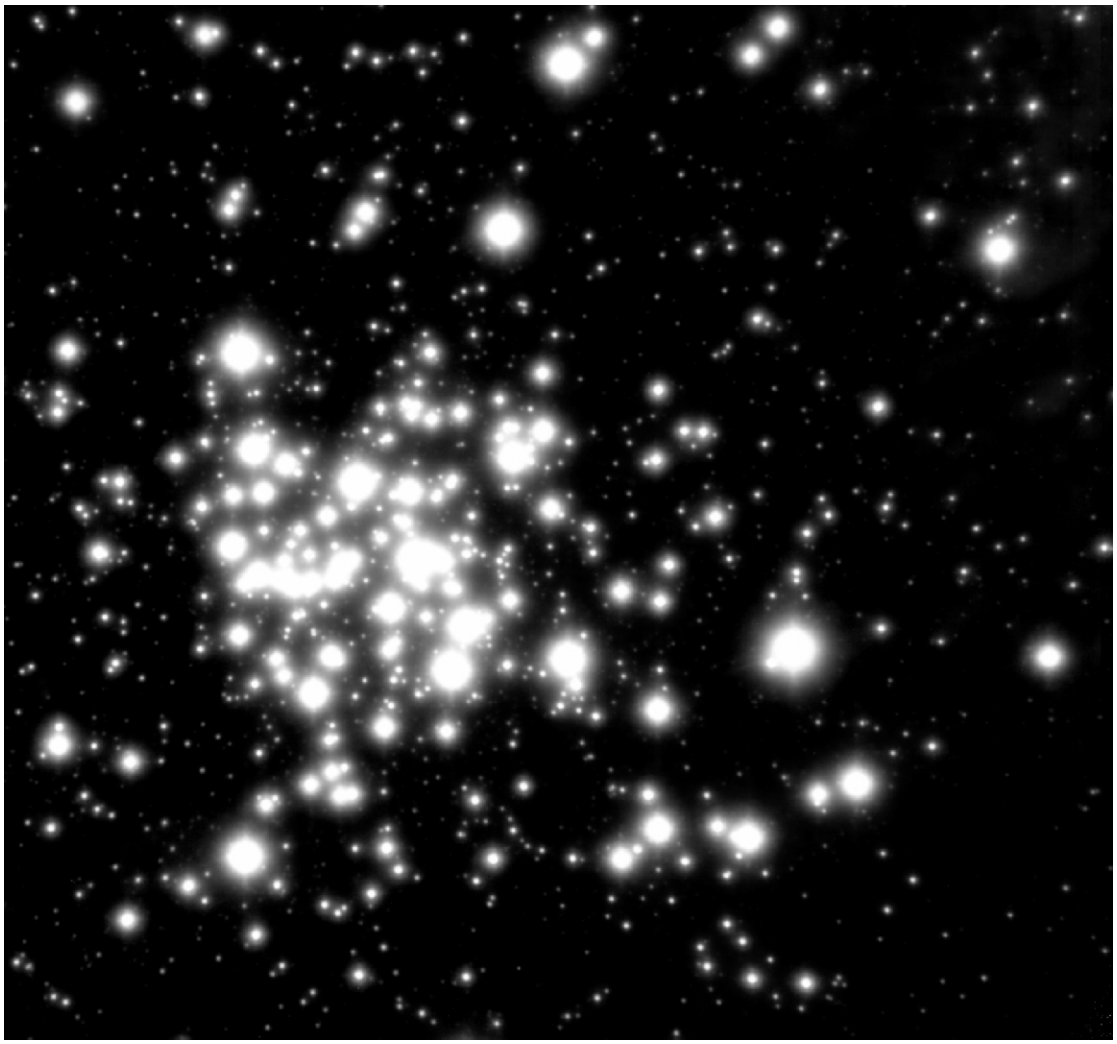


FIG. 1.—NACO combined *HK* image of the Arches cluster. The field of view is 24″ × 24″ with a final resolution of 0.″084. North is up, and east is to the left. [*See the electronic edition of the Journal for a color version of this figure*.]